

Scavenger Decapping Activity Facilitates 5' to 3' mRNA Decay

Hudan Liu and Megerditch Kiledjian*

Department of Cell Biology and Neuroscience, Rutgers University, 604 Allison Road,
Piscataway, New Jersey 08854-8082

Received 30 June 2005/Returned for modification 8 August 2005/Accepted 1 September 2005

mRNA degradation occurs through distinct pathways, one primarily from the 5' end of the mRNA and the second from the 3' end. Decay from the 3' end generates the m⁷GpppN cap dinucleotide, which is subsequently hydrolyzed to m⁷Gp and ppN in *Saccharomyces cerevisiae* by a scavenger decapping activity termed Dcs1p. Although Dcs1p functions in the last step of mRNA turnover, we demonstrate that its activity modulates earlier steps of mRNA decay. Disruption of the *DCS1* gene manifests a threefold increase of the *TIF51A* mRNA half-life. Interestingly, the hydrolytic activity of Dcs1p was essential for the altered mRNA turnover, as Dcs1p, but not a catalytically inactive Dcs1p mutant, complemented the increased mRNA stability. Mechanistic analysis revealed that 5' to 3' exoribonucleolytic activity was impeded in the *dcs1Δ* strain, resulting in the accumulation of uncapped mRNA. These data define a new role for the Dcs1p scavenger decapping enzyme and demonstrate a novel mechanism whereby the final step in the 3' mRNA decay pathway can influence 5' to 3' exoribonucleolytic activity.

A unique characteristic of eukaryotic mRNA is the N⁷-methylated guanosine cap structure that is cotranscriptionally added to the 5' terminus of nascent RNA (40). The cap serves to protect the 5' end of the mRNA from exoribonucleolytic degradation (49). It also functions in the transport of mature mRNA from the nucleus to the cytoplasm (18, 20), in translation initiation (12), and in pre-mRNA splicing (24). The cap is bound by distinct cap-binding proteins in each cellular compartment. A heterodimeric complex of CBC20 and CBC80 binds the cap in the nucleus (19), while eIF4E, the translation initiation factor, associates with the cap in the cytoplasm (12). In addition to these major cap binding proteins, several other factors have also been demonstrated to bind the mRNA cap, including the mammalian poly(A)-binding protein (22), the cold shock protein YB-1 (10), and the scavenger decapping protein (28, 37).

Decay of mRNA is not a randomized process and proceeds through at least two major decay pathways, both of which are initiated by removal of the poly(A) tail (31). Following deadenylation, the mRNA is decapped and degraded by a 5' to 3' exoribonucleolytic activity in the 5' decay pathway. In the 3' decay pathway, the mRNA is continuously degraded from the 3' end following deadenylation, generating an m⁷GpppN cap dinucleotide that is hydrolyzed by a scavenger decapping activity (27, 48).

Each mRNA decay pathway utilizes a unique decapping activity with a distinct substrate specificity (7). In the 5' pathway, both the yeast and human Dcp2 proteins utilize capped mRNA as a substrate and hydrolyze the cap structure to generate m⁷GDP and RNA with a monophosphate at its 5' end (29, 41, 43, 47). The exposed 5' end of the RNA is degraded by Xrn1p, the 5' to 3' exoribonuclease, leading to rapid degradation of the RNA body (4, 17, 25). A scavenger decapping activity termed DcpS in mammals and Dcs1p in budding yeast

functions in the final step of the 3' decay pathway. This activity hydrolyzes the residual cap structure following 3' to 5' exonucleolytic decay by the exosome complex to release m⁷GMP and nucleotide diphosphate (27, 48). Characterization of scavenger decapping activity indicates its strong preference for binding and hydrolyzing cap structure linked to an RNA of less than 10 nucleotides in mammals and 3 nucleotides in *Caenorhabditis elegans* (6, 27, 28).

Recent structural analysis of DcpS reveals that it can form either an asymmetric dimer bound to two cap dinucleotides (13) or a symmetric dimer in the ligand-free protein (5). The dimers contain distinct amino-terminal and carboxyl-terminal domains separated by a hinge region (13). The structure indicates that the N terminus can flip back and forth, alternating on each side from a productive closed to a nonproductive open conformation (13). An interesting property of DcpS is its almost exclusive utilization of the residual cap dinucleotide following 3' exonucleolytic decay of the RNA (27, 28). This substrate specificity is due in part to a higher affinity of DcpS for the cap structure (28) and more significantly to both entropic and steric constraints in the formation of a closed decapping-competent complex in the presence of an mRNA moiety on the cap (13).

Saccharomyces cerevisiae contains two proteins termed Dcs1p and Dcs2p that are equally homologous to the human DcpS. Curiously, only Dcs1p possesses intrinsic decapping activity analogous to that of DcpS (27). The enzymatic activity and substrate specificity for Dcs2p remain unknown, although its ability to heterodimerize with Dcs1p suggests that it might be a modulator of Dcs1p decapping activity (30). Dcs1p is a member of the histidine triad (HIT) family of nucleotide binding proteins and contains the characteristic HIT motif (His-X-His-X-His-X, where X is a hydrophobic amino acid) which is required for its cap hydrolysis activity (27). By virtue of its ability to hydrolyze the cap dinucleotide (27), DcpS and Dcs1p are postulated to function during the terminal phase of mRNA decay. Here we demonstrate that Dcs1p also functions to impact the 5' mRNA decay pathway.

* Corresponding author. Mailing address: Department of Cell Biology and Neuroscience, Rutgers University, 604 Allison Road, Piscataway, NJ 08854-8082. Phone: (732) 445-0796. Fax: (732) 445-0104. E-mail: kiledjian@biology.rutgers.edu.

TABLE 1. Strains used in this study

Strain	Genotype	Source
BY4742	<i>MAT</i> α <i>his3</i> Δ 1 <i>leu2</i> Δ 0 <i>lys2</i> Δ 0 <i>ura3</i> Δ 0	27
Y15179	<i>MAT</i> α <i>his3</i> Δ 1 <i>leu2</i> Δ 0 <i>lys2</i> Δ 0 <i>ura3</i> Δ 0 <i>dcs1::KanMX4</i>	27
Y12429	<i>MAT</i> α <i>his3</i> Δ 1 <i>leu2</i> Δ 0 <i>lys2</i> Δ 0 <i>ura3</i> Δ 0 <i>dcs2::KanMX4</i>	27
Y262	<i>MAT</i> α <i>ura3-52 his4-539 rpb1-1</i>	34
Y262 <i>dcs1</i> Δ	<i>MAT</i> α <i>ura3-52 his4-539 rpb1-1 dcs1::KanMX4</i>	This study
yRP684	<i>MAT</i> α <i>trp1-Δ1 ura3-52 leu2-3,112 his4-539</i>	4
yRP1192	<i>MAT</i> α <i>trp1-Δ1 ura3-52 leu2-3,112 his4-539 ski2::LEU2</i>	2
yRP1192 <i>dcs1</i> Δ	<i>MAT</i> α <i>trp1-Δ1 ura3-52 leu2-3,112 his4-539 ski2::LEU2 dcs1::KanMX4</i>	This study
yRP685	<i>MAT</i> α <i>trp1-Δ1 ura3-52 leu2-3,112 his4-539</i>	4
yJC135	<i>MAT</i> α <i>trp1-Δ1 ura3-52 leu2-3,112 his4-539 dhh1::URA3</i>	8
yJC135 <i>dcs1</i> Δ	<i>MAT</i> α <i>trp1-Δ1 ura3-52 leu2-3,112 his4-539 dhh1::URA3 dcs1::KanMX4</i>	This study

MATERIALS AND METHODS

Strains. Disruption of the *DCS1* gene within the Y262, yRP1192, and yJC135 backgrounds was carried out by homologous recombination using a cassette of the neomycin resistance gene flanked by *DCS1* extragenic sequences. The cassette was PCR amplified using the 5' primer (5' CATGTCCAAGAACATCG AAGAC 3') and the 3' primer (5' ATTCTTCAAATCTATGGCAGTCC 3') from the genomic DNA of strain Y15179 (ResGen Invitrogen Corporation, Huntsville, AL) containing a substitution of the neomycin resistance gene in the *DCS1* gene. All the strains used in this report are listed in Table 1.

Plasmids. The plasmid pRS426-DCS1, containing the full-length *DCS1* gene including 342 bp upstream of the translation start site and 488 bp downstream of the stop codon, was generated in two steps. The genomic sequence was amplified from BY4742 cells with primers 5' CCCTGAGAGCTCACGTCACCCCATCAT CCCACAT 3' and 5' CCCTGATCTAGACCTGAAAGTGATGGTAGATGT G 3' and inserted into the pCRII-TOPO (Invitrogen, Carlsbad, CA) plasmid. The fragment was subsequently excised with EcoRI and XhoI and ligated into the same sites of pRS426 (1). The plasmid pRS426-DCS1^M, encoding the *DCS1* gene with a site-specific substitution that converts the central histidine within the HIT motif to asparagine, was generated using a QuikChange mutagenesis system (Stratagene) with the following primers: 5' CTTCTTATTATCATTTCACCA TTCACATCGTTAAACATAAAG 3' and 5' CTTTATGTAAACGATGTGAAT GTTGAAATGATAAATAAGAAG 3'. The mutation was confirmed by sequencing. Plasmid transformations into yeast cells were carried out using YEAST-MAKER yeast transformation system 2 according to the protocol of the manufacturer (BD Biosciences, Palo Alto, CA) and maintained by growth in selective medium.

Extract preparation. Yeast total extract was prepared according to the method of Zhang et al. (50) with minor modifications. Cells were disrupted with glass beads by vortexing sequentially for 30 s each time followed by a 2-min cooling on ice repeated six times. After the extract was centrifuged at 10,000 \times g for 10 min to remove cellular debris, the supernatant was subjected to ultracentrifugation at 50,000 \times g for 45 min. The resulting supernatant was collected and supplemented with 10% glycerol, and protein concentrations were determined with Bio-Rad assay reagent (Bio-Rad Laboratories Inc., Hercules, CA).

Extraction of RNA and cDNA synthesis. Preparation of total RNA was performed according to Sarmientos et al. (39) by use of a hot phenol extraction method. Briefly, the cell pellet was resuspended in AE buffer (50 mM NaOAc [pH 5.3], 10 mM EDTA), extracted with phenol at 65°C for 10 min, and precipitated with 100% ethanol. cDNA was synthesized from total RNA with M-MLV reverse transcription (Invitrogen, Carlsbad, CA) according to the manufacturer's instructions, using random hexamer primers (Applied Biosystems, Foster City, CA).

Real-time PCR. mRNA expression levels were quantified from reverse-transcribed cDNA by real-time PCR using SYBR green PCR core reagent (Applied Biosystems, Foster City, CA), and *TIF51A*, *HTB1*, or *PGK1* mRNA abundance was quantitated using the standard curve method according to the recommendations of the manufacturer. Values were normalized to the stable *U3* RNA. Each gene was amplified using the appropriate specific primers, 5' ACCCAT AGCGGAGATGATG 3' and 5' TGAACATGGACGGTGACACT 3' for *TIF51A*, 5' CAAACTCACCTGACACTGG 3' and 5' TACGCAGCCAATTT AGAAGC 3' for *HTB1*, 5' GTTCCAGAAAGGTCGATGGTCA 3' and 5' CCG AAGGCATCGTTGATGTAA 3' for *PGK1*, and 5' GAGCCACTGAATCCA ACTTGGT 3' and 5' ATAGATGCCGAACCGCTAAG 3' for *U3*. For other experiments (see Fig. 4B), two sets of primers were simultaneously used to detect the two ends of the *TIF51A* mRNA. The presence of the 5' end of *TIF51A*

mRNA was detected with 5' GCTTCCTTTCCTTCTTTCTA 3' and 5'GGT ATGTTCTTCGTGACAGACA 3', while the 3' end was detected with primers 5'AGAAGCCGCCATCTCCT 3' and 5' GGGCGTCGGAGTTTTTTTT 3'. Real-time PCR was carried out with an ABI Prism 7900HT sequence detection system, and the specificity of the amplified PCR products was assessed by a melting curve analysis after the last cycle by the manufacturer's suggested program.

Cap antibody immunoprecipitations and Northern blotting. Immunoprecipitation of capped mRNA was carried out as described previously (15). Briefly, 20 μ g total RNA was incubated with agarose-conjugated 2,2,7-trimethyl-guanosine antibody (Calbiochem, San Diego, CA) for three rounds in IPPL buffer (150 mM NaCl, 10 mM Tris-HCl [pH 7.5], 1 mM EDTA, 0.05% NP-40, 1 mM dithiothreitol, 0.1 μ M RNasin) at 4°C. This antibody has previously been shown to efficiently immunopurify monomethyl capped mRNA (15). RNAs associated with the beads were eluted with IPPL buffer in the presence of 1% sodium dodecyl sulfate. RNA in the supernatant and elution was extracted with phenol-chloroform, precipitated with 100% ethanol, and resolved with a 1.25% formaldehyde agarose gel. The blot was probed with a DNA fragment corresponding to the *TIF51A* 3' untranslated region (3'UTR) labeled using Ready-To-Go DNA labeling beads (Amersham, NJ) in the presence of [α -³²P]dCTP.

Determination of poly(A) tail length. A poly(A) assay to detect the length of the *TIF51A* poly(A) tail was carried out as described previously (38) with slight modifications. Oligo(dT) anchor primer 5' GCGAGCTCCGCGGCCGCGTTT TTTTTTTTT 3' was used for reverse transcription. Amplification of the *TIF51A* 3' end was carried out by PCR with the 5' GTTATTTATCATCTATAG CAATAATATACTTTG 3' primer, the 5' primer, and the oligo(dT)-anchored 3' primer in the presence of [α -³²P]dATP. PCR amplified material was visualized by autoradiography following electrophoresis on a 6% 7 M urea denaturing polyacrylamide gel.

Generation of cap-labeled RNA and detection of decapping products. Uncapped *TIF51A* 3'UTR was transcribed in vitro with T7 polymerase from a PCR-generated template using the following primers: 5' CGTAATACGACT CACTATAGGGACCGGTTAACATCATGGCAT 3' and 5' CCCCCCCCC CCCCCCGAATAAAAACAAAGTATATTATTG 3'. Cap-labeled RNA containing the label on the first phosphate following the methyl guanosine (m⁷G*pppG-) was generated with the vaccinia virus capping enzyme utilizing [α -³²P]GTP and S-adenosyl-methionine, followed by gel purification as described previously (46). Decapping assays were carried out as previously described (27), and decapping products were resolved by polyethyleneimine-cellulose thin-layer chromatography (TLC) and developed in 0.45 M (NH₄)₂SO₄. The TLC plates (Sigma) were dried and detected with a Molecular Dynamics PhosphorImager (Storm 860).

Western blot analysis. Protein samples were resolved on 12.5% SDS gels and transferred to a nitrocellulose membrane (Schleicher & Schuell BioScience, Inc., Keene, NH) by use of a semidry blotting apparatus. Hybridizations were performed with affinity-purified human DcpS antibody (1:200) (27) and visualized by enhanced chemiluminescence using horseradish peroxidase-conjugated goat anti-rabbit secondary antibody (Cappel, West Chester, PA) (1:10,000 dilution).

[³⁵S]methionine incorporation. Yeast cells (100 ml culture) were grown in medium lacking methionine at 25°C to an optical density at 600 nm (OD₆₀₀) of 0.5, followed by supplementation with 50 μ M unlabeled methionine and 1 μ Ci/ml of [³⁵S]methionine (NEN). At each indicated time point (see Fig. 3), 1 ml of culture was removed for OD₆₀₀ analysis, and another 1 ml of cells was used for protein analysis by lysis and precipitation with 10% ice-cold trichloroacetic acid (TCA). The samples were filtered through 0.2 μ M nitrocellulose filters (Milli-

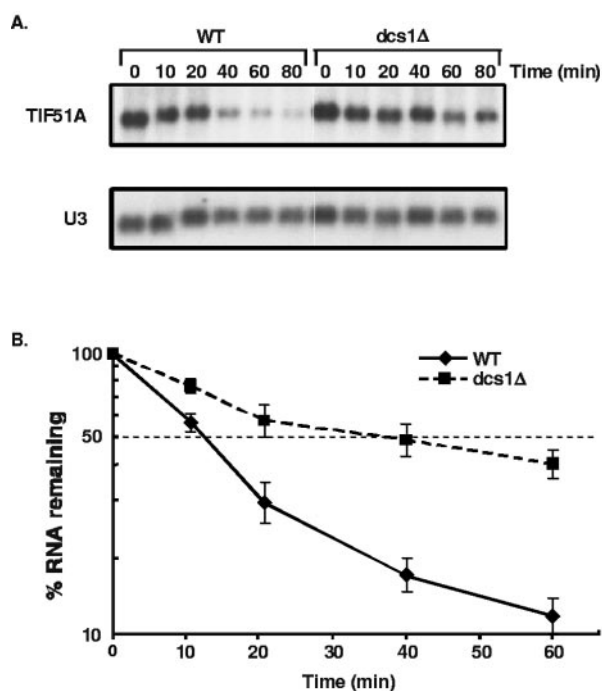


FIG. 1. Disruption of the Dcs1p scavenger decapping enzyme in *Saccharomyces cerevisiae* increases the stability of *TIF51A* mRNA. Degradation of *TIF51A* mRNA was monitored following transcriptional shutoff with thiolutin (20 μ g/ml), and RNA was isolated at the indicated time points. (A) Degradation of *TIF51A* transcripts was detected by Northern blot analysis. Time points following transcriptional repression are shown above the lanes. The top panel shows the results for the *TIF51A* mRNAs from isogenic wild-type (WT) (BY4742) and *dcs1* Δ (Y15179) cells. The blot was probed with 32 P-labeled *TIF51A* 3'UTR. The stable *U3* RNA was used as an internal control and, as shown in the bottom panel, probed with the entire coding sequence. (B) Half-life measurements of *TIF51A* transcripts were carried out by quantitative real-time PCR using RNA derived from wild-type and *dcs1* Δ strains as described for panel A. The numbers at the bottom indicate minutes after transcriptional repression. The percentage of RNA remaining at each time point was calculated, normalized to *U3* RNA levels by a standard curve method, and plotted for each time point. The average value and standard deviation at each time point were obtained from at least four independent experiments, each carried out in triplicate.

pore, Billerica, MA) prewashed with 5% TCA to retain the proteins. The filters were subsequently washed twice with 5 ml ice-cold 5% TCA to remove unincorporated [35 S]methionine and air dried. The amount of bound newly synthesized proteins was determined with a liquid scintillation counter.

RESULTS

Disruption of *DCS1* results in stabilization of the *TIF51A* mRNA. The scavenger decapping activity functions in the last step of the 3' mRNA decay pathway (27, 48). To address whether the last step of mRNA decay can influence the overall rate of mRNA turnover, we determined the consequence of the absence of Dcs1p on mRNA decay in a *DCS1*-disrupted yeast strain. The half-life of the *TIF51A* mRNA was monitored following transcriptional arrest with thiolutin. Interestingly, the stability of *TIF51A* mRNA was different in the two strains and threefold greater in the *dcs1* Δ strain, as determined by Northern blot analysis (Fig. 1A). The half-life increased from 13 min

in the wild-type strain to 40 min in the *dcs1* Δ strain. Similar results were also obtained using a quantitative real-time PCR approach with primers that amplified a fragment within the coding region of the *TIF51A* mRNA (Fig. 1B). These data demonstrate that the *TIF51A* mRNA is more stable in the *dcs1* Δ strain and suggest that Dcs1p contains a novel function that influences the efficiency of mRNA decay. Furthermore, the correlation between the Northern blot analysis and the quantitative real-time PCR analysis demonstrates the validity of the PCR approach, which was used in subsequent experiments.

The increase in *TIF51A* mRNA stability in *dcs1* Δ was not unique to thiolutin-mediated shutdown of transcription. A similar threefold difference was also observed in the *rpb1-1* strain background (Table 2; Fig. 2A), which contains a thermosensitive allele of the largest subunit of RNA polymerase II and allows inhibition of transcription under nonpermissive conditions (37°C) (16, 34). These data also demonstrate that the observed increase in *TIF51A* mRNA half-life upon disruption of the *DCS1* gene is not strain specific. The *rpb1-1* strain background is different from that used in Fig. 1. Furthermore, the increase in mRNA stability in the *dcs1* Δ strain was not restricted to the *TIF51A* mRNA only and was also observed with at least two other transcripts tested. The stability of the *HTB1* mRNA was also increased by threefold in the *dcs1* Δ strain relative to that of the parental strain from a half-life of 8 min to 23 min, respectively (Table 2). Similarly, the half-life of the stable *PGK1* transcript was greater than the 60-min duration of the experiment compared to 20 min seen with the parental strain (Table 2). These data suggest the observed increase of mRNA stability in the *dcs1* Δ strain is not restricted to a single transcript and could be a more general property.

Regulation of *TIF51A* mRNA stability is dependent on Dcs1p hydrolysis activity. To address whether the difference in *TIF51A* mRNA half-life was a function of the presence of Dcs1p, the *dcs1* Δ strain was complemented with the *DCS1* gene. As expected, the threefold increase of *TIF51A* mRNA half-life in the *DCS1*-disrupted background was reversed upon complementation with the *DCS1* gene (Fig. 2A). However, reversal of the increased half-life was not detected with a catalytically inactive Dcs1p mutant (Dcs1p^M) (Fig. 2A). Decapping assays using extract from cells complemented with the wild-type and mutant *DCS1* genes confirmed that strains complemented with the wild-type gene but not those complemented with the mutant gene contained decapping activity (data not shown). The mutant protein used harbored an asparagine substituted in place of histidine 268 within the HIT hydrolase motif to generate a decapping-deficient protein. Western blot analysis was carried out to confirm that the wild-type and mutant exogenous Dcs1p proteins were expressed at

TABLE 2. Increased mRNA stability in *dcs1* Δ strains

Strain	mRNA half-life (min)	
	<i>rpb1-1</i>	<i>rpb1-1 dcs1</i> Δ
HTB1	8	23
TIF51A	10	30
PGK1	20	60

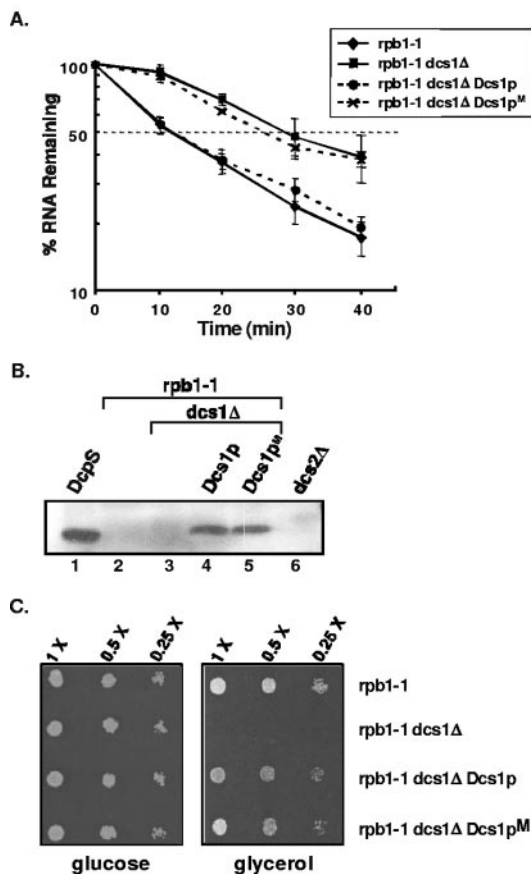


FIG. 2. Hydrolysis activity of Dcs1p is required to regulate the rate of *TIF51A* mRNA degradation. (A) Half-life measurements were assessed for the temperature-sensitive *rpb1-1* (Y262) strain. Transcription was repressed by a shift to the nonpermissive temperature of 37°C, and RNA was isolated at the indicated time points. The four different strains used are shown in the boxed insert. Dcs1p^M denotes the catalytically inactive mutant Dcs1p harboring a histidine-to-asparagine amino acid substitution (H268N) in the HIT motif. The average value and standard deviations for each time point were obtained from at least three independent experiments, each carried out in triplicate. (B) Expression of exogenous wild-type and inactive Dcs1p mutant was detected by Western blot analysis, utilizing primary antibody directed against human DcpS. With the amount of extract used in this experiment, there is enough cross-reactivity with the yeast Dcs1p protein to detect the overexpressed but not the endogenous protein. Lane 1 is the positive control detecting the human DcpS protein in HeLa cell extract (50 μg). Lanes 2 to 6 contained 50 μg of yeast extract derived from the indicated strains. (C) Expression of both wild-type and mutant Dcs1p complements the glycerol lethality phenotype. Dilutions of the indicated cells were spotted onto plates lacking uracil and containing either glucose (left panel) or glycerol (right panel) as the carbon source. Rows *rpb1-1* and *rpb1-1 dcs1Δ* contained the pRS426 empty vector with URA3 marker. The *rpb1-1 dcs1Δ* Dcs1p and *rpb1-1 dcs1Δ* Dcs1p^M cells expressed the pRS426 plasmid encoding the wild-type and the mutant *DCSI* gene, respectively.

equivalent levels (Fig. 2B). Judging on the basis of the similarity of the crystal structures for the wild-type and the HIT motif mutant-containing mammalian DcpS proteins (5, 14), the structure of the mutant yeast protein should not be altered by the single amino acid substitution. This point was further substantiated by the ability of the Dcs1p^M expression to suppress the glycerol lethality of the *dcs1Δ* strain. Under glycerol con-

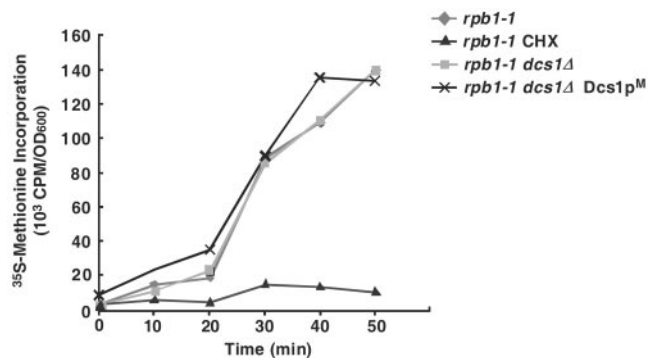


FIG. 3. Global translation efficiency remains unchanged in cells lacking expression of functional Dcs1p. Newly synthesized protein was labeled by [³⁵S]methionine incorporation. Cells were harvested at the indicated times following the addition of [³⁵S]methionine, and the level of incorporation was determined as described in Materials and Methods. The yeast strains used are listed in the insert. Where indicated, cycloheximide was included in the growth media at 100 μg/ml to block translation elongation. The values for the bound radioactive proteins were divided by the OD₆₀₀ reading and plotted relative to time.

ditions, both the wild-type and mutant Dcs1 proteins can complement the growth defect (Fig. 2C), further demonstrating that the overall structural integrity of the mutant protein is maintained. Taken together, these results indicate that functional Dcs1p was required for the regulation of *TIF51A* mRNA stability and strongly suggest that the hydrolytic activity, rather than the Dcs1p protein per se, serves the regulatory role.

The regulation of mRNA stability mediated by Dcs1p is independent of translation. Several observations argue that increasing mRNA association with ribosomes inhibits 5' decapping rates, which in turn slows mRNA decay. For example, inhibition of translation elongation by mutations or by elongation inhibitors significantly decreased the rates of 5' decapping (3, 36). To exclude the possibility that stabilization of *TIF51A* mRNA is a consequence of altered mRNA translation, we examined the global translation efficiency by determining the [³⁵S]methionine incorporation in cells possessing and lacking Dcs1p activity. Yeast cells were pulsed with [³⁵S]methionine, and newly synthesized proteins were detected. As shown in Fig. 3, the pattern of methionine incorporation over time in *dcs1Δ* was analogous to that obtained from the parental strain, while treatment with cycloheximide showed the expected inhibition of protein synthesis. These data demonstrate that there was no detectable defect in translation efficiency when Dcs1p was removed. *dcs1Δ* expressing the catalytically inactive Dcs1p^M also displayed normal translation (Fig. 3), confirming that loss of cap hydrolysis activity does not influence translation under these assay conditions. We conclude that the increase of mRNA stability observed in the *dcs1Δ* strain is not due to altered translation and is a direct consequence of scavenger decapping activity manifesting a novel regulatory mechanism.

Dcs1p activity influences 5' to 3' degradation of *TIF51A* mRNA. In an attempt to address the mechanism by which *TIF51A* mRNA became stabilized in the *dcs1Δ* background, we determined which step of mRNA decay was negatively impacted. The three most likely events include either the initial

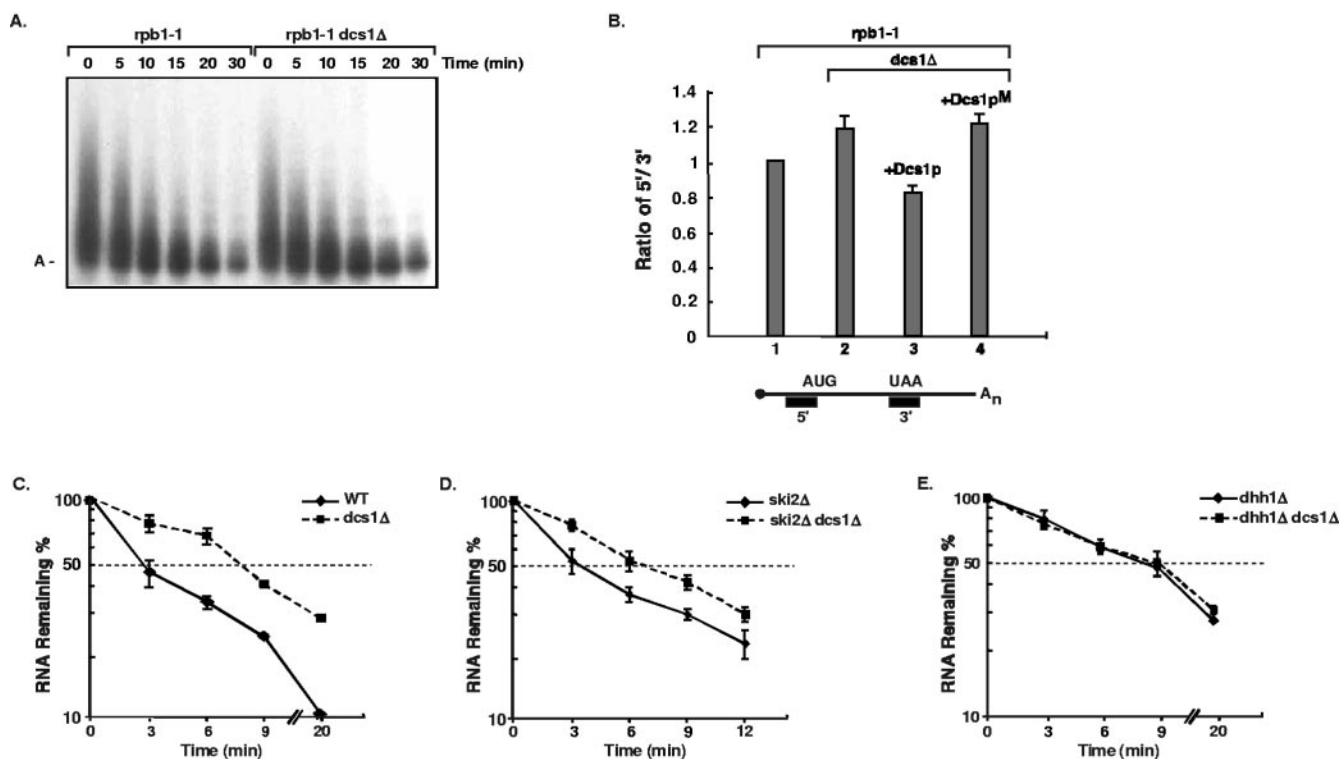


FIG. 4. Disruption of *DCS1* impedes 5' to 3' degradation of the *TIF51A* mRNA. (A) The length of the poly(A) tail in cells expressing or lacking Dcs1p was analyzed by the poly(A) assay. RNA was isolated from the two different strains at the indicated times following transcriptional repression as described for Fig. 2. Migration of unadenylated (A-) RNAs is denoted on the left side of the panel. (B) A schematic of the *TIF51A* mRNA is shown at the bottom of the panel, with the translation start (AUG) and stop (UAA) sites denoted and the relative position of the detected 5' and 3' fragments of the RNA indicated. The bar graph represents the relative steady-state ratios of the 5' to 3' fragments of the *TIF51A* RNA for each indicated strain as obtained by quantitative real-time PCR analysis. The 5' to 3' fragment ratios are presented relative to the ratio for the *rpb1-1* strain, which was arbitrarily set to 1. The values were derived from three independent experiments carried out in triplicate, with the error bars shown. (C) The half-life of the *TIF51A* mRNA measured by real-time PCR is shown in the isogenic wild-type (WT) (yRP684) and *dcs1Δ* strains. (D) The half-life of the *TIF51A* mRNA for *ski2Δ* (yRP1192) and *ski2Δ dcs1Δ* strains is shown as determined by the same approach used as described for panel C. (E) Half-life measurements for the *TIF51A* mRNA are shown for *dhh1Δ* (yJC135) and *dhh1Δ dcs1Δ* cells as determined by the same approach used as described for panel C. The transcriptional block and normalization relative to the *U3* RNA for panels C, D, and E were carried out as described in the legend to Fig. 1. Note that the differences in *TIF51A* mRNA half-lives observed in Fig. 1, 2, and 4 are a function of the different strain backgrounds used.

deadenylation step or one of the subsequent 5' to 3' or 3' to 5' decay steps. As shown in Fig. 4A, comparable deadenylation rates were detected for the *TIF51A* mRNA following transcriptional shutoff between strains expressing and lacking *DCS1*. The decrease in poly(A) tail length over time was indistinguishable between the wild-type and *dcs1Δ* cells by a poly(A) assay (38), suggesting that there was no significant effect on deadenylation in the absence of Dcs1p.

Having ruled out an influence at the level of deadenylation as the cause for the greater stability of the *TIF51A* mRNA, we next determined whether decay from either the 5' or 3' end was affected. Several complementary approaches were used to address this question. A modification of an approach we previously used to simultaneously monitor the disappearance of both termini of an mRNA was employed (48). The presence of sequences at the 5' end of *TIF51A* mRNA relative to sequences corresponding to the 3' end was detected using quantitative real-time PCR. We would anticipate a ratio of the two termini to be approximately 1, since the majority of mRNAs would be either full length or completely degraded. However, a small percentage of mRNAs that were in the midst of decay

from one end or the other would be trapped upon RNA isolation. These intermediates would skew the ratio to more than 1 under conditions that stabilize the 5' end or to less than 1 when the 3' end is more stable. A comparison of the 5'-to-3' ratio between the *rpb1-1* and the *rpb1-1 dcs1Δ* strains revealed that a ratio greater than 1 (Fig. 4B, bars 1 and 2) indicated that the 5' end of the *TIF51A* mRNA was more stable in the absence of *DCS1*. The increased prevalence of the 5' end in the *dcs1Δ* background was a consequence of Dcs1p, as complementation with the *DCS1* gene reversed the increase (Fig. 4B, bar 3). The greater stability of the 5' end of the *TIF51A* mRNA is a function of Dcs1p activity and is not directly determined by the protein, since the catalytically inactive Dcs1p^M was unable to complement the increased stability of the 5' end (Fig. 4B, bar 4). These data imply that the 5' decay pathway is influenced by the hydrolytic activity of Dcs1p.

A complementary genetic approach with mutants that crippled either the 5' or the 3' decay pathway was also utilized to more definitively address whether the Dcs1p influence was mediated through the 5' decay pathway. Dhh1p is a putative RNA helicase that facilitates decapping by the Dcp1p/2p de-

capping complex, and the decapping step is severely compromised in a *dhh1Δ* background (8, 11). If the repression of *TIF51A* mRNA degradation were mediated through the 5' decay pathway, the *TIF51A* mRNA stability in cells harboring either a *dhh1Δ* disruption or a *dhh1Δ dcs1Δ* double disruption should remain the same, since the 5' decay pathway is already compromised. Conversely, a double disruption of *dcs1Δ* with *ski2Δ*, which is essential for the decay of an mRNA from the 3' end (2), would be expected to result in an additive stabilization.

We first confirmed that disruption of the *DCS1* gene, within the parental strain from which the *DHH1* and *SKI2* gene lesions were derived, maintained the observed increase in *TIF51A* mRNA stability. As shown in Fig. 4C, a threefold-greater half-life was detected in this strain background upon disruption of the *DCS1* gene. Consistent with 5' end decay being a critical determinant for the *TIF51A* mRNA decay (45), a block of the 3' decay pathway in the *ski2Δ* strain did not significantly alter the *TIF51A* mRNA half-life relative to that of the parental strain (3.5 min compared to 2.5 min, respectively). As expected, the stability of *TIF51A* mRNA was increased in the *ski2Δ dcs1Δ* double-disruption cells compared to the *ski2Δ* strain results (Fig. 4D). These data demonstrate an additive effect of *dcs1Δ* and *ski2Δ* on *TIF51A* mRNA stability. Consistent with an influence of Dcs1p on 5' end decay, the *TIF51A* mRNA half-life was not significantly altered in the presence or absence of the *DCS1* gene within the *dhh1Δ* background (Fig. 4E). Collectively, these data indicate that the Dcs1p influence is exerted through the 5' decay pathway.

Dcs1p activity regulates 5' to 3' exoribonucleolytic activity. Having determined that Dcs1p imparts a regulatory influence on the 5' decay pathway, we next addressed which step was altered. The influence of Dcs1p could be through either the 5' decapping step or the subsequent 5' to 3' exoribonucleolytic step, both of which were tested. Extract derived from either wild-type or *dcs1Δ* cells was utilized in an in vitro decapping assay using cap-labeled *TIF51A* 3'UTR RNA substrate. Dcp1p/2p decapping activity was detected in the cytoplasmic 50,000 × *g* supernatant fraction (S50) (Fig. 5A, lane 3). The presence of m⁷GDP was confirmed by its conversion to m⁷GTP by nucleotide diphosphate kinase (NDPK) (48) (lanes 5 and 6). A comparison of lanes 3 and 4 demonstrates similar levels of decapping efficiency, as determined by the generation of m⁷GDP. Therefore, the presence or absence of Dcs1p did not appear to have a significant effect on mRNA decapping under these in vitro assay conditions.

Following decapping of the deadenylated mRNA, the RNA is degraded by the 5' to 3' exoribonuclease Xrn1p in yeast (17). To address whether this exoribonucleolytic step is hindered in the *dcs1Δ* cells, we determined whether uncapped RNA accumulated in the disrupted strain. Uncapped RNA would not be detected under wild-type conditions due to efficient exoribonucleolytic decay, while accumulation of this substrate was detected in an *xrn1Δ* background (15, 32, 51). Therefore, if the exoribonuclease step were slowed in the *dcs1Δ* strain, we would expect uncapped RNA to accumulate. Capped RNA was separated from uncapped RNA by immunoprecipitation with an anticap antibody, and the presence of *TIF51A* RNA was monitored. The reaction was spiked with ³²P-cap-labeled RNA to determine the efficiency of capped RNA immunoprecipitation. As shown in the control panel on the bottom of Fig. 5B, capped

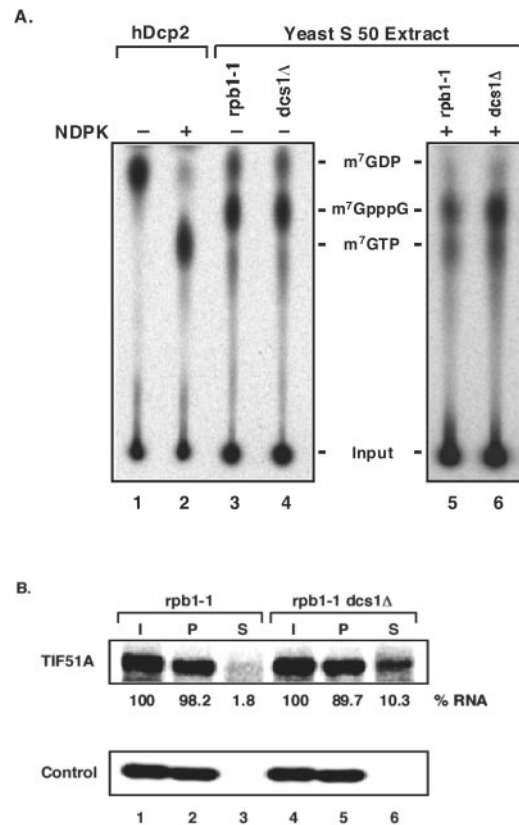


FIG. 5. 5' exonucleolytic activity is compromised in *dcs1Δ* strains. (A) In vitro decapping assays were carried out by incubating cap-labeled (m⁷G*pppG-) *TIF51A* 3'UTR RNA with yeast S50 extract (20 μg) from cells containing (lane 3) or lacking (lane 4) scavenger decapping activity. 100 μM m⁷GpppG was added to each reaction mixture to sequester Dcs1p activity and allow detection of m⁷GDP formation. The decapping products were resolved by TLC in 0.45 M (NH₄)₂SO₄. Recombinant human Dcp2 was used as a marker for m⁷GDP production (lane 1). To confirm the presence of m⁷GDP, the products from lane 1, 3, and 4 were treated with NDPK and resolved in lanes 2, 5, and 6, respectively. NDPK converts m⁷GDP to m⁷GTP (48). Standards were developed on the TLC simultaneously and visualized by UV shadowing, and their migration is indicated between the two panels. (B) Uncapped RNA accumulates in the *dcs1Δ* strain. Aliquots (20 μg) of total RNA isolated from the indicated yeast strains were immunoprecipitated utilizing monoclonal antitrimethylguanosine antibody. The pellet (P) lanes contain immunoprecipitated RNA corresponding to capped RNA. The results for the supernatant of the immunoprecipitation corresponding to uncapped RNA (S) and an aliquot of input RNA (I) are shown. The RNAs were resolved in denaturing formaldehyde agarose gel, and the presence of *TIF51A* mRNA was subjected to Northern analysis. Quantitations for the percentages of RNA were derived from three independent experiments. The reaction mixtures were spiked with ³²P cap-labeled RNA to assess the efficiency of the immunoprecipitations (bottom panel).

RNA was detected only in the immunoprecipitated fraction but not in the supernatant fraction. This observation confirms the efficiency of the capped RNA immunoprecipitation and demonstrates that the antibody was not saturated with capped RNA under these assay conditions.

The immunoprecipitated RNAs were next detected by Northern blot analysis to detect the proportion of capped versus uncapped *TIF51A* RNA. In wild-type cells, 98% of *TIF51A* RNA was capped and present in the immunoprecipitated lane

whereas the supernatant fraction, corresponding to uncapped RNA, contained only a trace amount of *TIF51A* RNA (Fig. 5B; compare lane 2 to 3). In contrast, 10% of uncapped RNA was detected in the *dcs1Δ* cells (lane 6), demonstrating that uncapped RNA accumulates in the *dcs1Δ* strain. This result was reproducible with three independent experiments. Collectively, our results imply that 5' exoribonucleolytic activity is positively regulated by Dcs1p in yeast cells. Therefore, stability of the *TIF51A* mRNA is increased due to a hindrance of the 5' to 3' exoribonucleolytic activity in the absence of the scavenger decapping function.

DISCUSSION

We present a novel role for the scavenger decapping enzyme in mRNA degradation in *Saccharomyces cerevisiae*. Dcs1p, which was previously thought to function primarily in the last step of mRNA decay (27, 44), also influences overall mRNA stability (Fig. 1, 2A, and 4C; Table 2). Furthermore, we demonstrate that this regulation is at the level of 5' to 3' exoribonucleolytic decay (Fig. 4 and 5). Although our analysis focused on the *TIF51A* mRNA, a similar stabilization was observed in the *dcs1Δ* strain for two other mRNAs tested, the *PGK1* and *HTB1* mRNAs, demonstrating that this regulation is not restricted to *TIF51A*. Our data support the hypothesis that Dcs1p functions in a general regulatory mechanism whereby its activity influences the degradation of mRNA in the 5' decay pathway.

Several lines of evidence support the role of Dcs1p in a potential feedback mechanism regulating the stability of mRNA by influencing 5' end decay. First, strains disrupted for *DCS1* contain mRNAs that are more stable than strains that express *DCS1* (Fig. 1, 2A, and 4C; Table 2), indicating that Dcs1p influences mRNA decay. Second, the 5' end of the *TIF51A* mRNA persisted longer than the 3' end in the absence of functional Dcs1p, a result which was subsequently reversed upon expression of active Dcs1p (Fig. 4B). Third, genetic inactivation of the 5' degradation pathway abolished the Dcs1p-mediated effect on mRNA decay (Fig. 4D). Lastly, uncapped *TIF51A* mRNA accumulated in the absence of Dcs1p activity, indicating that the 5' to 3' exoribonuclease activity involved in the decay of uncapped mRNA is compromised (Fig. 5B). Considering that Xrn1p is the cytoplasmic exoribonuclease responsible for 5'-end decay of mRNA in yeast (17, 21, 31), it is most likely that Dcs1p activity influences Xrn1p function (Fig. 6).

In addition to the interesting finding that a Dcs1p-mediated function exists to regulate 5' exoribonucleolytic decay, an unexpected result was that this regulation was dependent on the decapping activity of Dcs1p but not directly dependent on the Dcs1p protein. This was made evident by the observed complementation of the *dcs1Δ* strain with Dcs1p but not the catalytically inactive Dcs1p^M protein containing a single amino acid substitution in the HIT motif active site (Fig. 2A and 4B). These data indicate that the regulator is not a protein that is directly controlled by Dcs1p through protein-protein interactions; rather, either the substrate or product of Dcs1p could be functioning as a signal to influence overall mRNA decay.

We propose that Dcs1p can influence mRNA decay by controlling the availability of its m⁷GpppN cap dinucleotide substrate or its hydrolyzed methylated guanosine product (Fig. 6).

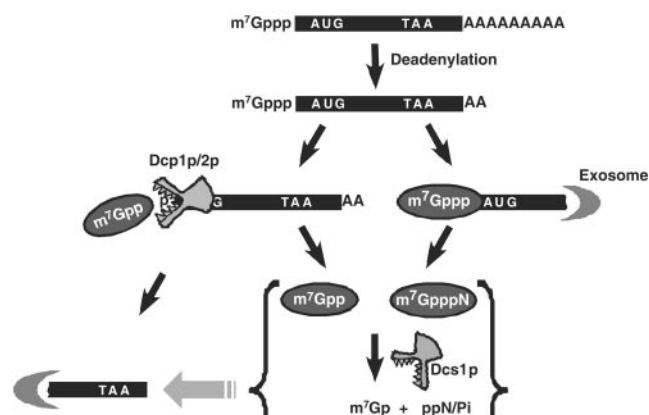


FIG. 6. Model of the *Saccharomyces cerevisiae* scavenger decapping activity feedback regulation of mRNA decay. Following deadenylation, the mRNA can be degraded from the 5' end through a decapping step carried out by the Dcp1p/2p complex to release m⁷GDP and the exposed 5' end hydrolyzed by Xrn1p. Alternatively, the RNA continues to degrade from the 3' end by the exosome complex, generating a cap dinucleotide, m⁷GpppN. Both m⁷GDP and m⁷GpppN can be hydrolyzed by Dcs1p to m⁷GMP, which is subsequently dephosphorylated to m⁷G. In the absence of Dcs1p, the two substrates would be expected to accumulate whereas formation of the products would be expected to decrease. The observed stability of mRNA thought to be mediated through Xrn1p could be due to either an inhibitory effect of one or both of the Dcs1p substrates or a stimulatory effect of one or both of the Dcs1p products.

Yeast disrupted for the *DCS1* gene accumulate m⁷GpppN cap dinucleotide (27), which could serve as a negative effector of 5' to 3' exoribonuclease activity. A role for Dcs1p as a regulator of dinucleotide levels is consistent with previous suggestions that HIT protein family members could be mediators of dinucleotide signaling molecules (23, 26). Conversely, m⁷GMP, the Dcs1p decapping product, or m⁷G, the subsequent dephosphorylated product, could serve as a positive effector of exoribonuclease activity. In the absence of Dcs1p, the lack of m⁷GMP (or m⁷G) could lead to a slowing of exoribonuclease activity.

It is presently unclear whether the cap dinucleotide or the decapping product serves as the signal influencing mRNA decay. However, since m⁷GMP is a general mRNA decay product, it could function as the signal. m⁷GMP can be formed by Dcs1p in cells by the hydrolysis of m⁷GpppN (27), m⁷GDP (44), and m⁷GTP (unpublished observations). Further support for m⁷GMP, rather than the cap dinucleotide, as the mediator comes from Fig. 4D, in which it is shown that stability of the *TIF51A* mRNA was greater in the *ski2Δ dcs1Δ* double disruption than in the *ski2Δ* single disruption. Considering that the *ski2Δ* strain is compromised in 3'-end exonucleolytic decay, we would expect minimal, if any, cap dinucleotide accumulation. However, m⁷GMP would still be generated from the Dcp2p product of m⁷GDP, which can be hydrolyzed to m⁷GMP by Dcs1p (44). Therefore, the observed additive effect in the *ski2Δ dcs1Δ* double-disruption strain supports the hypothesis that mRNA stabilization results from the lack of m⁷GMP formation.

One surprising finding of our work is that the feedback regulation is at the level of exoribonuclease decay rather than at the level of the initial decapping step. Although at present the physiological implication is unclear, a coordination be-

tween the two exonucleolytic decay pathways appears most likely. The ability of the scavenger decapping activity to enhance 5' exonucleolytic decay could serve to facilitate the rapid clearing of uncapped mRNAs. Accumulation of uncapped mRNA could otherwise sequester exosome protein components and prevent their function on capped mRNAs that are destined for decay and need to be cleared. The activity of the exosome on capped mRNAs, which are still translationally competent, might be more critical than its function on uncapped RNAs that are translationally incompetent. Whether Dcs1p can coordinate this interplay remains to be determined.

Although it has long been thought to be among the least-regulated steps of mRNA decay, several examples exist showing that the 5' to 3' exoribonuclease step is regulated. First, the *TIF51A* gene product has been shown to specifically influence 5' exoribonucleolytic activity following decapping (51). Second, accumulation of pAp in cells results in the inhibition of Xrn1p exoribonuclease activity (9). Further underscoring the significance of 5' exoribonucleolytic activity, the expression of Xrn1 is developmentally controlled in *Drosophila melanogaster* (42) and critical for ventral epithelial enclosure during embryogenesis in *C. elegans* (33). Modulation of 5' to 3' exoribonuclease activity could also regulate the decay of mRNA fragments generated by small interfering RNA-mediated cleavage which involves Xrn1 in both *C. elegans* (33) and *D. melanogaster* (35). Our study provides additional evidence that the 5' to 3' exoribonuclease activity can be modulated and is more regulated than previously appreciated.

A second surprising finding of this work is the demonstration that Dcs1p is a multifunctional protein that functions in a role independent of its decapping activity. Disruption of the *DCS1* gene results in a slow-growth phenotype under glucose conditions and a lethal phenotype when glycerol is used as the carbon source (Fig. 2C). Interestingly, the catalytically inactive Dcs1p^M, which is unable to reverse the increased mRNA stability in the *dcs1Δ* cells, was nevertheless able to complement the glycerol lethality (Fig. 2C). These data demonstrate that the decapping activity of Dcs1p and its influence on mRNA decay can be uncoupled from novel function in glycerol-dependent growth.

Our data support a more general role for the yeast scavenger decapping activity in mRNA turnover. In addition to its function in clearing the cap structure during terminal stages of mRNA decay, it also impacts earlier steps involving 5' to 3' exonucleolytic decay. In its absence, the 5' to 3' exoribonuclease activity is compromised but not completely blocked. Current efforts are focused on understanding the mechanism by which 5' to 3' exonucleolytic decay is controlled by the scavenger decapping activity.

ACKNOWLEDGMENTS

We thank D. Cao, J. Collier, A. van Hoof, and R. Parker for providing yeast strains and Pfizer for providing thiolutin. We also thank G. Qing, R. Duttgupta, C. Martin, T. Kinzy, R. Hart, A. Jacobson, and members of the Kiledjian laboratory for helpful discussions.

This work was supported by National Institutes of Health grant GM67005 to M.K.

REFERENCES

- Anand, M., K. Chakraborty, M. J. Marton, A. G. Hinnebusch, and T. G. Kinzy. 2003. Functional interactions between yeast translation eukaryotic elongation factor (eEF) 1A and eEF3. *J. Biol. Chem.* **278**:6985–6991.

- Anderson, J. S. J., and R. Parker. 1998. The 3' to 5' degradation of yeast mRNAs is a general mechanism for mRNA turnover that requires the SKI2 DEVH box protein and 3' to 5' exonucleases of the exosome complex. *EMBO J.* **17**:1497–1506.
- Beelman, C. A., and R. Parker. 1994. Differential effects of translational inhibition in *cis* and *trans* on the decay of the unstable yeast MFA2 mRNA. *J. Biol. Chem.* **269**:9687–9692.
- Beelman, C. A., A. Stevens, G. Caponigro, T. E. LaGrandeur, L. Hatfield, D. M. Fortner, and R. Parker. 1996. An essential component of the decapping enzyme required for normal rates of mRNA turnover. *Nature* **382**:642–646.
- Chen, N., M. A. Walsh, Y. Liu, R. Parker, and H. Song. 2005. Crystal structures of human DcpS in ligand-free and m7GDP-bound forms suggest a dynamic mechanism for scavenger mRNA decapping. *J. Mol. Biol.* **347**:707–718.
- Cohen, L. S., C. Mikhli, C. Friedman, M. Jankowska-Anyszka, J. Stepinski, E. Darzynkiewicz, and R. E. Davis. 2004. Nematode m7GpppG and m3(2,2,7)GpppG decapping: activities in *Ascaris* embryos and characterization of *C. elegans* scavenger DcpS. *RNA* **10**:1609–1624.
- Coller, J., and R. Parker. 2004. Eukaryotic mRNA decapping. *Annu. Rev. Biochem.* **73**:861–890.
- Coller, J. M., M. Tucker, U. Sheth, M. A. Valencia-Sanchez, and R. Parker. 2001. The DEAD box helicase, Dhh1p, functions in mRNA decapping and interacts with both the decapping and deadenylase complexes. *RNA* **7**:1717–1727.
- Dichl, B., A. Stevens, and D. Tollervey. 1997. Lithium toxicity in yeast is due to the inhibition of RNA processing enzymes. *EMBO J.* **16**:7184–7195.
- Evdokimova, V., P. Ruzanov, H. Imataka, B. Raught, Y. Svitkin, L. P. Ovchinnikov, and N. Sonenberg. 2001. The major mRNA-associated protein YB-1 is a potent 5' cap-dependent mRNA stabilizer. *EMBO J.* **20**:5491–5502.
- Fischer, N., and K. Weis. 2002. The DEAD box protein Dhh1 stimulates the decapping enzyme Dcp1. *EMBO J.* **21**:2788–2797.
- Gingras, A. C., B. Raught, and N. Sonenberg. 1999. eIF4 initiation factors: effectors of mRNA recruitment to ribosomes and regulators of translation. *Annu. Rev. Biochem.* **68**:913–963.
- Gu, M., C. Fabrega, S. W. Liu, H. Liu, M. Kiledjian, and C. D. Lima. 2004. Insights into the structure, mechanism, and regulation of scavenger mRNA decapping activity. *Mol. Cell* **14**:67–80.
- Gu, M., and C. D. Lima. 2005. Processing the message: structural insights into capping and decapping mRNA. *Curr. Opin. Struct. Biol.* **15**:99–106.
- He, F., and A. Jacobson. 2001. Upf1p, Nmd2p, and Upf3p regulate the decapping and exonucleolytic degradation of both nonsense-containing mRNAs and wild-type mRNAs. *Mol. Cell. Biol.* **21**:1515–1530.
- Herrick, D., R. Parker, and A. Jacobson. 1990. Identification and comparison of stable and unstable mRNAs in *Saccharomyces cerevisiae*. *Mol. Cell. Biol.* **10**:2269–2284.
- Hsu, C. L., and A. Stevens. 1993. Yeast cells lacking 5'→3' exoribonuclease 1 contain mRNA species that are poly(A) deficient and partially lack the 5' cap structure. *Mol. Cell. Biol.* **13**:4826–4835.
- Izaurrealde, E., J. Lewis, C. Gamberi, A. Jarmolowski, C. McGuigan, and I. W. Mattaj. 1995. A cap-binding protein complex mediating U snRNA export. *Nature* **376**:709–712.
- Izaurrealde, E., J. Lewis, C. McGuigan, M. Jankowska, E. Darzynkiewicz, and I. W. Mattaj. 1994. A nuclear cap binding protein complex involved in pre-mRNA splicing. *Cell* **78**:657–668.
- Jarmolowski, A., W. C. Boelens, E. Izaurrealde, and I. W. Mattaj. 1994. Nuclear export of different classes of RNA is mediated by specific factors. *J. Cell Biol.* **124**:627–635.
- Johnson, A. W. 1997. Rat1p and Xrn1p are functionally interchangeable exoribonucleases that are restricted to and required in the nucleus and cytoplasm, respectively. *Mol. Cell. Biol.* **17**:6122–6130.
- Khanna, R., and M. Kiledjian. 2004. poly(A)-binding-protein-mediated regulation of hDcp2 decapping in vitro. *EMBO J.* **23**:1968–1976.
- Kisselev, L. L., J. Justesen, A. D. Wolfson, and L. Y. Frolova. 1998. Diadenosine oligophosphates (Ap(n)A), a novel class of signalling molecules? *FEBS Lett.* **427**:157–163.
- Konarska, M. M., R. A. Padgett, and P. A. Sharp. 1984. Recognition of cap structure in splicing in vitro of mRNA precursors. *Cell* **38**:731–736.
- LaGrandeur, T. E., and R. Parker. 1998. Isolation and characterization of Dcp1p, the yeast mRNA decapping enzyme. *EMBO J.* **17**:1487–1496.
- Lee, Y. N., H. Nechushtan, N. Figov, and E. Razin. 2004. The function of lysyl-tRNA synthetase and Ap4A as signaling regulators of MITF activity in FeRI-activated mast cells. *Immunity* **20**:145–151.
- Liu, H., N. D. Rodgers, X. Jiao, and M. Kiledjian. 2002. The scavenger mRNA decapping enzyme DcpS is a member of the HIT family of pyrophosphatases. *EMBO J.* **21**:4699–4708.
- Liu, S. W., X. Jiao, H. Liu, M. Gu, C. D. Lima, and M. Kiledjian. 2004. Functional analysis of mRNA scavenger decapping enzymes. *RNA* **10**:1412–1422.
- Lykke-Andersen, J. 2002. Identification of a human decapping complex as-

- sociated with hUpf proteins in nonsense-mediated decay. *Mol. Cell. Biol.* **22**:8114–8121.
30. **Malys, N., K. Carroll, J. Miyan, D. Tollervey, and J. E. McCarthy.** 2004. The 'scavenger' m7GpppX pyrophosphatase activity of Dcs1 modulates nutrient-induced responses in yeast. *Nucleic Acids Res.* **32**:3590–3600.
 31. **Meyer, S., C. Temme, and E. Wahle.** 2004. Messenger RNA turnover in eukaryotes: pathways and enzymes. *Crit. Rev. Biochem. Mol. Biol.* **39**:197–216.
 32. **Muhrad, D., and R. Parker.** 1994. Premature translational termination triggers mRNA decapping. *Nature* **370**:578–581.
 33. **Newbury, S., and A. Woollard.** 2004. The 5'-3' exoribonuclease xrn-1 is essential for ventral epithelial enclosure during *C. elegans* embryogenesis. *RNA* **10**:59–65.
 34. **Nonet, M., C. Scafe, J. Sexton, and R. Young.** 1987. Eucaryotic RNA polymerase conditional mutant that rapidly ceases mRNA synthesis. *Mol. Cell. Biol.* **7**:1602–1611.
 35. **Orban, T. L., and E. Izaurralde.** 2005. Decay of mRNAs targeted by RISC requires XRN1, the Ski complex, and the exosome. *RNA* **11**:459–469.
 36. **Peltz, S. W., and A. Jacobson.** 1992. mRNA stability: in trans-it. *Curr. Opin. Cell Biol.* **4**:979–983.
 37. **Salehi, Z., L. Geffers, C. Vilela, R. Birkenhager, M. Ptushkina, K. Berthelot, M. Ferro, S. Gaskell, I. Hagan, B. Stapley, and J. E. McCarthy.** 2002. A nuclear protein in *Schizosaccharomyces pombe* with homology to the human tumour suppressor Fhit has decapping activity. *Mol. Microbiol.* **46**:49–62.
 38. **Salles, F. J., W. G. Richards, and S. Strickland.** 1999. Assaying the polyadenylation state of mRNAs. *Methods* **17**:38–45.
 39. **Sarmientos, P., J. E. Sylvester, S. Contente, and M. Cashel.** 1983. Differential stringent control of the tandem *E. coli* ribosomal RNA promoters from the *rrnA* operon expressed in vivo in multicopy plasmids. *Cell* **32**:1337–1346.
 40. **Shatkin, A. J.** 1976. Capping of eucaryotic mRNAs. *Cell* **9**:645–653.
 41. **Steiger, M., A. Carr-Schmid, D. C. Schwartz, M. Kiledjian, and R. Parker.** 2003. Analysis of recombinant yeast decapping enzyme. *RNA* **9**:231–238.
 42. **Till, D. D., B. Linz, J. E. Seago, S. J. Elgar, P. E. Marujo, M. L. Elias, C. M. Arraiano, J. A. McClellan, J. E. McCarthy, and S. F. Newbury.** 1998. Identification and developmental expression of a 5'-3' exoribonuclease from *Drosophila melanogaster*. *Mech. Dev.* **79**:51–55.
 43. **van Dijk, E., N. Cougot, S. Meyer, S. Babajko, E. Wahle, and B. Seraphin.** 2002. Human Dcp2: a catalytically active mRNA decapping enzyme located in specific cytoplasmic structures. *EMBO J.* **21**:6915–6924.
 44. **van Dijk, E., H. Le Hir, and B. Seraphin.** 2003. DcpS can act in the 5'-3' mRNA decay pathway in addition to the 3'-5' pathway. *Proc. Natl. Acad. Sci. USA* **100**:12081–12086.
 45. **Vasudevan, S., and S. W. Peltz.** 2001. Regulated ARE-mediated mRNA decay in *Saccharomyces cerevisiae*. *Mol. Cell* **7**:1191–1200.
 46. **Wang, Z., N. Day, P. Trifillis, and M. Kiledjian.** 1999. An mRNA stability complex functions with poly(A)-binding protein to stabilize mRNA in vitro. *Mol. Cell. Biol.* **19**:4552–4560.
 47. **Wang, Z., X. Jiao, A. Carr-Schmid, and M. Kiledjian.** 2002. The hDcp2 protein is a mammalian mRNA decapping enzyme. *Proc. Natl. Acad. Sci. USA* **99**:12663–12668.
 48. **Wang, Z., and M. Kiledjian.** 2001. Functional link between the mammalian exosome and mRNA decapping. *Cell* **107**:751–762.
 49. **Wilusz, C. J., M. Wormington, and S. W. Peltz.** 2001. The cap-to-tail guide to mRNA turnover. *Nat. Rev. Mol. Cell Biol.* **2**:237–246.
 50. **Zhang, S., C. J. Williams, M. Wormington, A. Stevens, and S. W. Peltz.** 1999. Monitoring mRNA decapping activity. *Methods* **17**:46–51.
 51. **Zuk, D., and A. Jacobson.** 1998. A single amino acid substitution in yeast eIF-5A results in mRNA stabilization. *EMBO J.* **17**:2914–2925.